ScienceFrontier
Research Article
Biomedical Research and Clinical Advancements
ISSN Online: 3065-341X | OPEN ACCESS

Analysis and Control of Zika Transmission Dynamic Models

Abstract:
The Zika virus is most commonly spread to people by the bite of an infected *Aedes* species mosquito. It can also be spread through sex from a person who is infected with Zika virus to their sexual partner(s). Zika virus can be passed from a pregnant woman to her fetus. Infection during pregnancy can cause certain birth defects. Zika virus typically occurs in tropical and subtropical areas of Africa, the Americas, Southern Asia, and the Western Pacific. There is currently no vaccine to prevent or medicine to treat Zika. It is therefore important to understand the dynamics of the Zika virus and develop strategies to control the spread of this virus. In this work, bifurcation analysis and multiobjective nonlinear model predictive control is performed on two dynamic models involving Zika transmission. Bifurcation analysis is a powerful mathematical tool used to deal with the nonlinear dynamics of any process. Several factors must be considered, and multiple objectives must be met simultaneously. . The MATLAB program MATCONT was used to perform the bifurcation analysis. The MNLMPC calculations were performed using the optimization language PYOMO in conjunction with the state-of-the-art global optimization solvers IPOPT and BARON. The bifurcation analysis revealed the existence of a branch point in the first model and a Hopf bifurcation point and a limit point in the second. The Hopf bifurcation point, which causes an unwanted limit cycle, is eliminated using an activation factor involving the tanh function. The branch and limit points (which cause multiple steady-state solutions from a singular point) are very beneficial because they enable the Multiobjective nonlinear model predictive control calculations to converge to the Utopia point (the best possible solution) in the models.

Key Words: bifurcation; optimization; control; zika

Author Information

Lakshmi. N. Sridhar*
Chemical Engineering Department University of Puerto Rico Mayaguez

***Corresponding Author:** Lakshmi. N. Sridhar, Chemical Engineering Department University of Puerto Rico Mayaguez

Received Date: June 05, 2025; **Accepted Date:** June 11, 2025; **Published Date:** June 30, 2025

Citation: Lakshmi. N. Sridhar (2025). Analysis and Control of Dengue Transmission Dynamic Models, J *Biomedical Research and Clinical Advancements* . 2 (3) 25, **DOI**: BRCA-25-RA-25.

Introduction:

Duffy et al (2009)[1] , discussed the Zika virus outbreak on Yap Island. Haddow et al (2012)[2] , researched the genetic characterization of Zika virus strains. Oehler et al (2014)[3] demonstrated the Zika virus infection complication by the Guillain-Barré syndrome. Bewick et al (2016)[4] discussed the endemic and epidemic dynamics of the Zika virus. Perkins et al (2016)[5] discussed the model-based projections of Zika virus infections in childbearing women in the Americas. Bogoch et al (2016)[6] discussed the international spread of Zika virus from Brazil. Bonyah et al (2016)[7] , developed a mathematical model of the

Zika virus. Brasil et al (2016)[[8] talked about the , zika virus infection in pregnant women. Cao-Lormeau et al (2016)[9] discussed the Guillain-Barré syndrome, outbreak associated with Zika virus infection. Cauchemez et al (2016)[10] , researched the association between the Zika virus and microcephaly. Elsaka et al (2016)[11] developed a fractional order network model for ZIKA. Fauci, et al (2016)[12]Zika virus spread in the Americas. Gao et al (2016)[13] discussed the prevention and control of Zika as a mosquito-borne and sexually transmitted disease. Heukelbach et al (2016)[14], discussed the Zika virus outbreak in Brazil.

Kucharski, et al (2016)[15] researched the transmission dynamics of Zika virus in island populations. Mlakar et al (2016)[16] demonstrated the association of the Zika virus with microcephaly. Lee et al (2016)[17] , developed a compartmental model for the zika virus with dynamic human and vector populations. Kibona et al (2017)[18] developed an SIR model involving the Zika virus infections and microcephaly. Boret et al (2017)[19] , developed a model of the zika virus in Brazil. Moreno et al (2017)[20] discussed the role of the short-term dispersal on the dynamics of Zika virus in an extreme idealized environment. Folashade et al (2017) [21] developed a mathematical model of the zika virus with vertical transmission. Suparit et al (2018)[22] developed a mathematical model for Zika virus transmission dynamics with a time-dependent mosquito biting rate. Wiratsudakul et al (2018)[23] studied the dynamics of Zika virus outbreaks with an overview of mathematical modelling approaches. Terefe et al (2018)[24] discussed the mathematics of a model for zika transmission dynamics. Blanka Tesla et al (2018)[25] showed how the temperature drives zika virus transmission. Khan et al (2019)[26] developed a dynamical model of asymptomatic carrier zika virus with optimal control strategies. Denu et al (2022)[27] developed an analysis and optimal control of a deterministic Zika virus model.

This work aims to perform bifurcation analysis and multiobjective nonlinear control (MNLMPC) studies in two Zika transmission models, which are discussed in Khan et al (2019)[26] (model 1) and Denu et al (2022)[27] (model 2). The paper is organized as follows. First, the model equations are presented, followed by a discussion of the numerical techniques involving bifurcation analysis and multiobjective nonlinear model predictive control (MNLMPC). The results and discussion are then presented, followed by the conclusions.

Model Equations:

Model 1Khan et al (2019)[26]

The variables (sh; eh; ih; rh; ah; sv; ev; iv) represent, the susceptible humans, exposed humans, asymptomatic carrier humans, infected humans ; recovered humans; susceptible mosquitoes; exposed mosquitoes; and infected mosquitoes.

The model equations are

$$\begin{aligned}
\frac{d(sh)}{dt} &= \Lambda_h - (b(nh)) - (\mu_h sh) - \left((1-u1)\beta_h sh\left((\rho(ih)) + iv\right)\right) \\
\frac{d(eh)}{dt} &= \left((1-u1)\beta_h sh\left((\rho(ih)) + iv\right)\right) - (\mu_h + \chi_h)eh) \\
\frac{d(ih)}{dt} &= (\varphi\chi_h eh) - \left(\left(\eta + \mu_h + (\gamma u2)\right)ih\right) \\
\frac{d(rh)}{dt} &= (\gamma u2ih) - (\mu_h rh) \\
\frac{d(ah)}{dt} &= \left((1-\varphi)\chi_h eh\right) - (\mu_h ah) \\
\frac{d(sv)}{dt} &= \left(\Lambda_v nv(1-u3)\right) - \left((1-u1)\beta_v sv(ih)\right) - (u3\mu_v sv) \\
\frac{d(ev)}{dt} &= \left((1-u1)\beta_v sv(ih)\right) - \left(\left((u3\mu_v) + \delta_v\right)ev\right) \\
\frac{d(iv)}{dt} &= (\delta_v ev) - (u3\mu_v iv) \\
nh &= sh + eh + ih + rh + ah \\
nv &= sv + ev + iv
\end{aligned} \tag{1}$$

u1; u2; and u3 are the control parameters.

The base parameter values are

$$\Lambda_h = 100; \beta_h = 0.02; \rho = 0.02; \mu_h = 4.0469e-05; \chi_h = 1/5; \varphi = 0.013;$$
$$\gamma = 0.001; \eta = 0.002; \Lambda_v = 0.02; \beta_v = 0.0002; \mu_v = 1/21; \delta_v = 1/10;$$
$$b = 0.001; u1 = 0.5; u2 = 0.5; u3 = 0.5;$$

Model 2 Denu et al (2022)[27]

In this model, x1, x2, x3, y1, and y2 represent the susceptible humans, the infectious humans, the recovered humans, the susceptible mosquitoes, and the infectious mosquitoes.

$$\begin{aligned}
\frac{d(x1)}{dt} &= (\delta_1) - \left(\frac{abx1y2*(1-u1)}{h}\right) - \left(\frac{\beta x1x2}{h}\right) - (\eta x1) \\
\frac{d(x2)}{dt} &= \left(\frac{abx1y2\theta(1-u1)}{h}\right) + \left(\frac{\beta x1x2\theta}{h}\right) - (\gamma x2) - (\eta x2) - u2 \\
\frac{d(x3)}{dt} &= \left(\frac{abx1y2(1-\theta)(1-u1)}{h}\right) + \left(\frac{\beta x1x2(1-\theta)}{h}\right) + (\gamma x2) - (\eta x3) + u2 \\
\frac{d(y1)}{dt} &= (\delta_2) - \left(\frac{acptx2y1*(1-u1)}{h}\right) - (vy1); \\
\frac{d(y2)}{dt} &= \left(\frac{acptx2y1(1-u1)}{h}\right) - (vy2) \\
h &= x1 + x2 + x3 \\
v &= y1 + y2
\end{aligned} \tag{2}$$

u1 and u2 are the control parameters. The base parameter values are

$$a = 0.4; b = 0.4; c = 0.3; \beta = 0.4; \theta = 0.8; \eta = 1/60; \gamma = 0.07; pt = 0.1;$$
$$\delta_1 = 2; \delta_2 = 4; u1 = 0.1; u2 = 0.2.$$

Bifurcation analysis

The MATLAB software MATCONT is used to perform the bifurcation calculations. Bifurcation analysis deals with multiple steady-states and limit cycles. Multiple steady states occur because of the existence of branch and limit points. Hopf bifurcation points cause limit cycles . A commonly used MATLAB program that locates limit points, branch points, and Hopf bifurcation points is MATCONT(Dhooge Govearts, and Kuznetsov, 2003[28]; Dhooge Govearts, Kuznetsov, Mestrom and Riet, 2004[29]). This program detects Limit points(LP), branch points(BP), and Hopf bifurcation points(H) for an ODE system

$$\frac{dx}{dt} = f(x, \alpha) \tag{3}$$

$x \in R^n$ Let the bifurcation parameter be α . Since the gradient is orthogonal to the tangent vector,

The tangent plane at any point $w = [w_1, w_2, w_3, w_4, ...w_{n+1}]$ must satisfy

$$Aw = 0 \tag{4}$$

Where A is

$$A = [\partial f / \partial x \quad | \partial f / \partial \alpha] \tag{5}$$

where $\partial f / \partial x$ is the Jacobian matrix. For both limit and branch points, the Jacobian matrix $J = [\partial f / \partial x]$ must be singular.

For a limit point, there is only one tangent at the point of singularity. At this singular point, there is a single non-zero vector, y, where Jy=0. This vector is of dimension n. Since there is only one tangent the vector $y=(y_1,y_2,y_3,y_4,...y_n)$ must align with $\hat{w}=(w_1,w_2,w_3,w_4,...w_n)$. Since

$$J\hat{w}=Aw=0 \tag{6}$$

the n+1 th component of the tangent vector w_{n+1} = 0 at a limit point (LP).

For a branch point, there must exist two tangents at the singularity. Let the two tangents be z and w. This implies that

$$\begin{aligned} Az&=0\\ Aw&=0 \end{aligned} \tag{7}$$

Consider a vector v that is orthogonal to one of the tangents (say w). v can be expressed as a linear combination of z and w ($v=\alpha z+\beta w$). Since $Az=Aw=0$; $Av=0$ and since w and v are orthogonal,

$w^Tv=0$. Hence $Bv=\begin{bmatrix}A\\ w^T\end{bmatrix}v=0$ which implies that B is singular.

Hence, for a branch point (BP) the matrix $B=\begin{bmatrix}A\\ w^T\end{bmatrix}$ must be singular.

At a Hopf bifurcation point,

$$\det(2f_x(x,\alpha)@I_n)=0 \tag{8}$$

@ indicates the bialternate product while I_n is the n-square identity matrix. Hopf bifurcations cause limit cycles and should be eliminated because limit cycles make optimization and control tasks very difficult. More details can be found in Kuznetsov (1998[30]; 2009[31]) and Govaerts [2000] [32].

Hopf bifurcations cause limit cycles. The tanh activation function (where a control value u is replaced by) $(u\tanh u/\varepsilon)$ is used to eliminate spikes in the optimal control profiles(Dubey et al 2022[33]; Kamalov et al, 2021[34] and Szandała, 2020[35];Sridhar 2023[36]). Sridhar (2024)[37] explained with several examples how the activation factor involving the tanh function also eliminates the Hopf bifurcation points. This was because the tanh function increases the oscillation time period in the limit cycle.

Multiobjective Nonlinear Model Predictive Control(MNLMPC)

The rigorous multiobjective nonlinear model predictive control (MNLMPC) method developed by Flores Tlacuahuaz et al (2012)[38] was used.

Consider a problem where the variables $\sum_{t_{i=0}}^{t_i=t_f} q_j(t_i)$ (j=1, 2..n) have to be optimized simultaneously for a dynamic problem

$$\frac{dx}{dt}=F(x,u) \tag{9}$$

t_f being the final time value, and n the total number of objective variables and u the control parameter. The single objective optimal control problem is solved individually optimizing each of the variables $\sum_{t_{i=0}}^{t_i=t_f} q_j(t_i)$ The optimization of

$\sum_{t_{i=0}}^{t_i=t_f} q_j(t_i)$ will lead to the values q_j^* . Then, the multiobjective optimal control (MOOC) problem that will be solved is

$$\min(\sum_{j=1}^{n}(\sum_{t_{i=0}}^{t_i=t_f} q_j(t_i) - q_j^*))^2 \qquad (10)$$
$$subject\ to\ \frac{dx}{dt} = F(x,u);$$

This will provide the values of u at various times. The first obtained control value of u is implemented and the rest are discarded. This procedure is repeated until the implemented and the first obtained control values are the same or if the Utopia point where ($\sum_{t_{i=0}}^{t_i=t_f} q_j(t_i) = q_j^*$ for all j) is obtained.

Pyomo (Hart et al, 2017)[39] is used for these calculations. Here, the differential equations are converted to a Nonlinear Program (NLP) using the orthogonal collocation method The NLP is solved using IPOPT (Wächter And Biegler, 2006)[40]and confirmed as a global solution with BARON (Tawarmalani, M. and N. V. Sahinidis 2005)[41].

The steps of the algorithm are as follows

1. Optimize $\sum_{t_{i=0}}^{t_i=t_f} q_j(t_i)$ and obtain q_j^*.
2. Minimize $(\sum_{j=1}^{n}(\sum_{t_{i=0}}^{t_i=t_f} q_j(t_i) - q_j^*))^2$ and get the control values at various times.
3. Implement the first obtained control values
4. Repeat steps 1 to 3 until there is an insignificant difference between the implemented and the first obtained value of the control variables or if the Utopia point is achieved. The Utopia point is when $\sum_{t_{i=0}}^{t_i=t_f} q_j(t_i) = q_j^*$ for all j.

Sridhar (2024)[42] demonstrated that when the bifurcation analysis revealed the presence of limit and branch points tthe MNLMPC calculations to converge to the Utopia solution . For this, the singularity condition, caused by the presence of the limit or branch points was imposed on the co-state equation (Upreti, 2013)[43]. If the minimization of q_1 lead to the value q_1^* and the minimization of q_2 lead to the value q_2^* The MNLPMC calculations will minimize the function $(q_1 - q_1^*)^2 + (q_2 - q_2^*)^2$. The multiobjective optimal control problem is

$$\min \quad (q_1 - q_1^*)^2 + (q_2 - q_2^*)^2 \quad subject\ to\ \frac{dx}{dt} = F(x,u) \qquad (11)$$

Differentiating the objective function results in

$$\frac{d}{dx_i}((q_1 - q_1^*)^2 + (q_2 - q_2^*)^2) = 2(q_1 - q_1^*)\frac{d}{dx_i}(q_1 - q_1^*) + 2(q_2 - q_2^*)\frac{d}{dx_i}(q_2 - q_2^*) \qquad (12)$$

The Utopia point requires that both $(q_1 - q_1^*)$ and $(q_2 - q_2^*)$ are zero. Hence

$$\frac{d}{dx_i}((q_1 - q_1^*)^2 + (q_2 - q_2^*)^2) = 0 \quad (13)$$

The optimal control co-state equation (Upreti; 2013)[43] is

$$\frac{d}{dt}(\lambda_i) = -\frac{d}{dx_i}((q_1 - q_1^*)^2 + (q_2 - q_2^*)^2) - f_x\lambda_i; \quad \lambda_i(t_f) = 0 \quad (14)$$

λ_i is the Lagrangian multiplier. t_f is the final time. The first term in this equation is 0 and hence

$$\frac{d}{dt}(\lambda_i) = -f_x\lambda_i; \lambda_i(t_f) = 0 \quad (15)$$

At a limit or a branch point, for the set of ODE $\frac{dx}{dt} = f(x,u)$ f_x is singular. Hence there are two different vectors-values for $[\lambda_i]$ where $\frac{d}{dt}(\lambda_i) > 0$ and $\frac{d}{dt}(\lambda_i) < 0$. In between there is a vector $[\lambda_i]$ where $\frac{d}{dt}(\lambda_i) = 0$. This coupled with the boundary condition $\lambda_i(t_f) = 0$ will lead to $[\lambda_i] = 0$ This makes the problem an unconstrained optimization problem, and the optimal solution is the Utopia solution.

Results and Discussion

The bifurcation analysis for Model 1 with u3 as the bifurcation parameter revealed a branch point (BP at (sh; eh; ih; rh; ah; sv; ev; iv; u3) values of (977.301174; 19.436982; 19.892451; 245.773933; 94809.862005; 0; 0; 0; 0.295775). This is seen in Fig. 1a.

For theMNLMPC calculations in model 1, sh(0) and sv(0) are (10000 and 1000 respectively. $\sum_{t_{i=0}}^{t_i=t_f} ah(t_i), \sum_{t_{i=0}}^{t_i=t_f} eh(t_i), \sum_{t_{i=0}}^{t_i=t_f} ih(t_i)$ were minimized individually and each of them led to a value of 0. 85, The overall optimal control problem will involve the minimization of $(\sum_{t_{i=0}}^{t_i=t_f} ah(t_i) - 0)^2 (\sum_{t_{i=0}}^{t_i=t_f} ih(t_i) - 0)^2 + (\sum_{t_{i=0}}^{t_i=t_f} eh(t_i) - 0)^2$ was minimized subject to the equations governing the model. This led to a value of zero (the Utopia solution. The various concentration profiles for this MNLMPC calculation are shown in Figs. 1b-1i.

The MNLMPC values of the control variables, u1 u2 u3 were 1, 0.4909, and 0.16934.

The noise exhibited by the control profiles (u1, u2, u3) (Fig. 1h) was remedied using the Savitzky Golay filter (Fig. 1i) to produce the control profiles (u1sg, u2sg, u3sg). It is seen that the presence of the branch point is beneficial because it allows the MNLMPC calculations to attain the Utopia solution, validating the analysis of Sridhar(2024)[42].

The bifurcation analysis for Model 2 with u2 as the bifurcation parameter revealed a Hopf bifurcation point and a limit point at (curve AB) (x1, x2, x3, y1, y2,u2) values (48.093182, 7.475539, 64.431279, 1.999327, 0.000673, 0.310878) and (62.448968, 4.607696, 52.943336, 1.999585, 0.000415, 0.368013). This is shown in Fig. 2a. When the manipulated variable u2 is changed to u2*tanh(u2)/0.015 the Hopf bifurcation point disappears (curve CD in Fig. 2a). This validates the analysis in Sridhar(2024)[37]. The limit cycle produced by this Hopf bifurcation point is shown in Fig. 2b.

For theMNLMPC calculations in model 2, x1(0) and y1(0) are (500 and 50 respectively. $\sum_{t_{i=0}}^{t_i=t_f} x2(t_i), \sum_{t_{i=0}}^{t_i=t_f} y2(t_i)$ were minimized individually and each of them led to a value of 0. The overall optimal control problem will involve the minimization of

$$(\sum_{t_{i=0}}^{t_i=t_f} x2(t_i)-0)^2(\sum_{t_{i=0}}^{t_i=t_f} y2(t_i)-0)^2$$

was minimized subject to the equations governing the model. This led to a value of zero (the Utopia solution. The various concentration profiles for this MNLMPC calculation are shown in Figs. 2c-2f.

The MNLMPC values of the control variables, u1 u2 were 0.1632, and 1.52e-05.

The noise exhibited by the control profiles (u1, u2) (Fig. 2e) was remedied using the Savitzky Golay filter (Fig. 2f) to produce the control profiles (u1sg, u2sg). It is observed that the presence of the branch point is beneficial, as it enables the MNLMPC calculations to attain the Utopia solution, thereby validating the analysis by Sridhar (2024)[42].

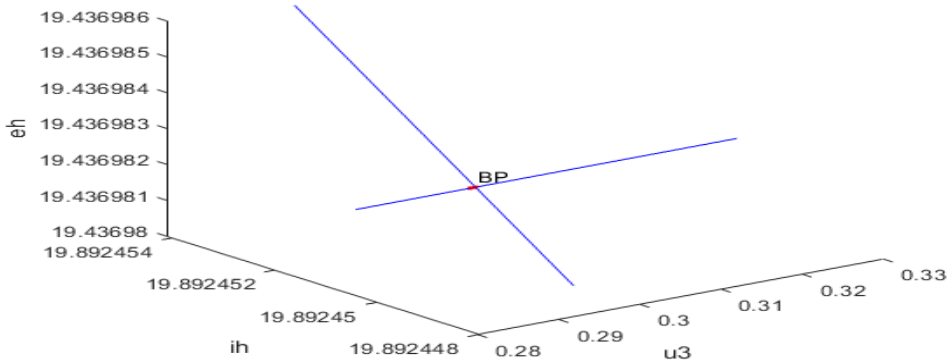

Figure 1a: *Bifurcation Diagram for Zika Model 1*

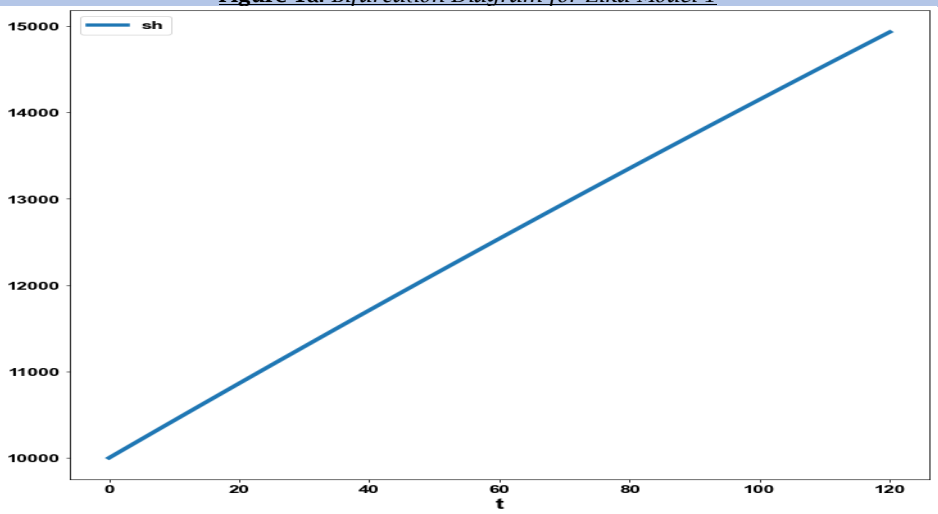

Figure 1b: *MNLMPC Zika Model 1(sh vs t)*

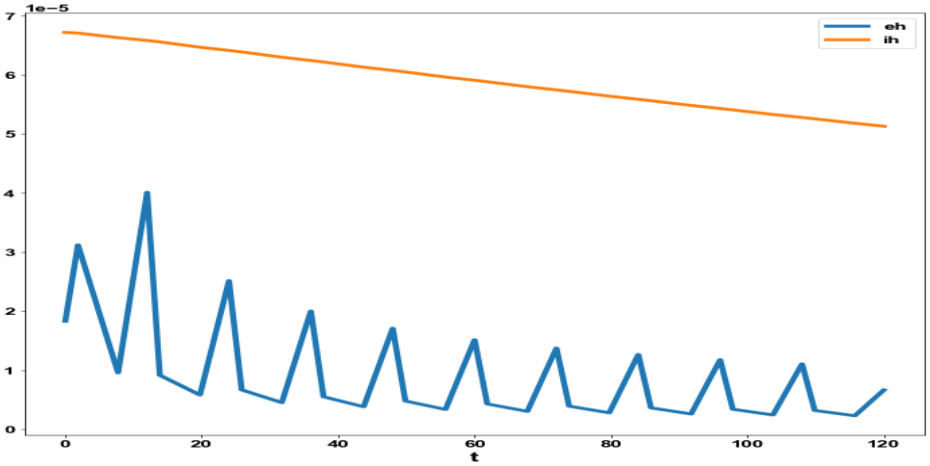

Figure 1c: *MNLMPC Zika Model 1(eh, ih vs t)*

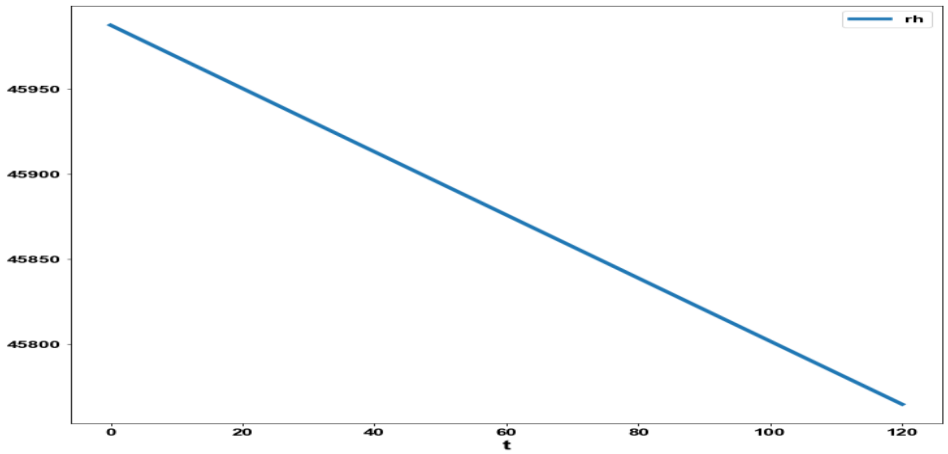

Figure 1d: *MNLMPC Zika Model 1 (rh vs t)*

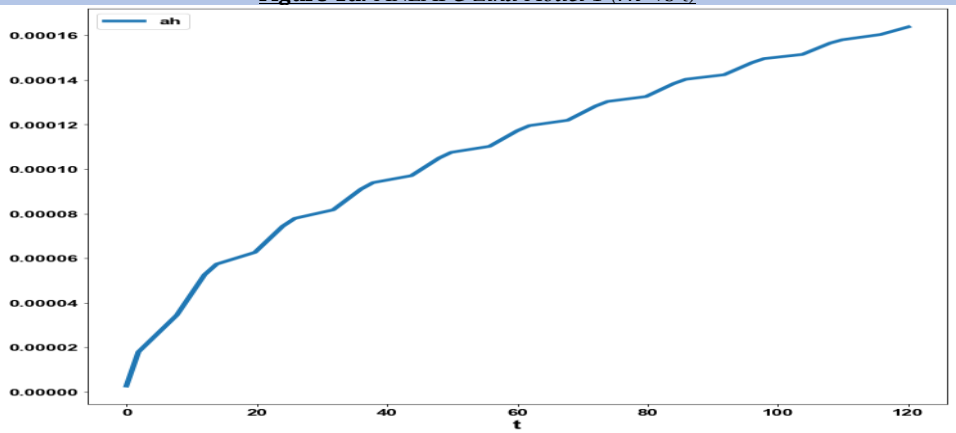

Figure 1e: *MNLMPC Zika Model 1 (eh vs t)*

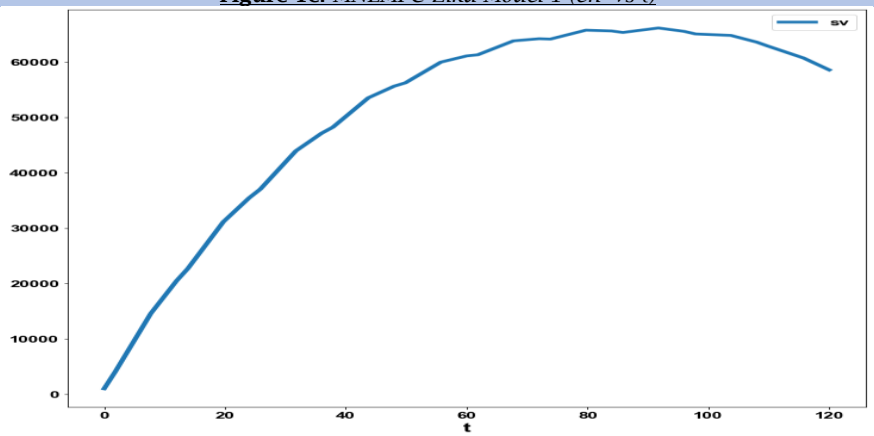

Figure 1f: *MNLMPC Zika Model 1 (sv vs t)*

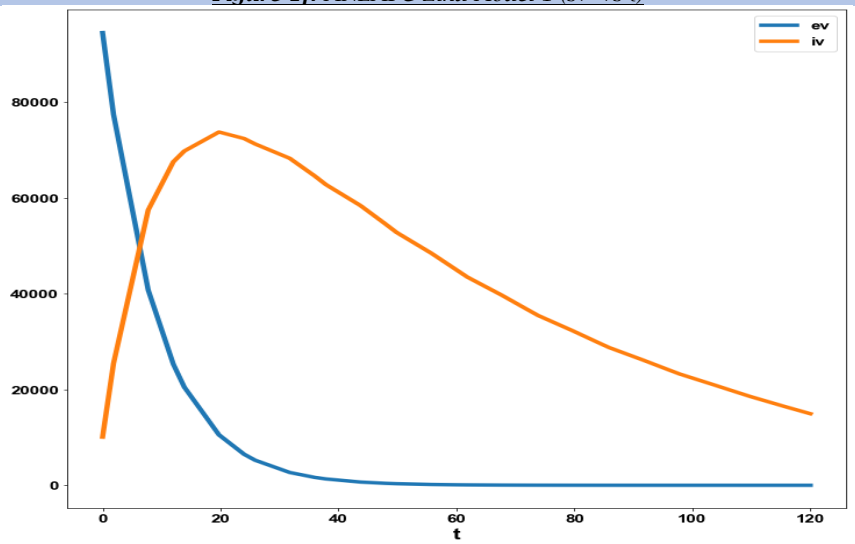

Figure 1g: *MNLMPC Zika Model 1 (ev,iv vs t)*

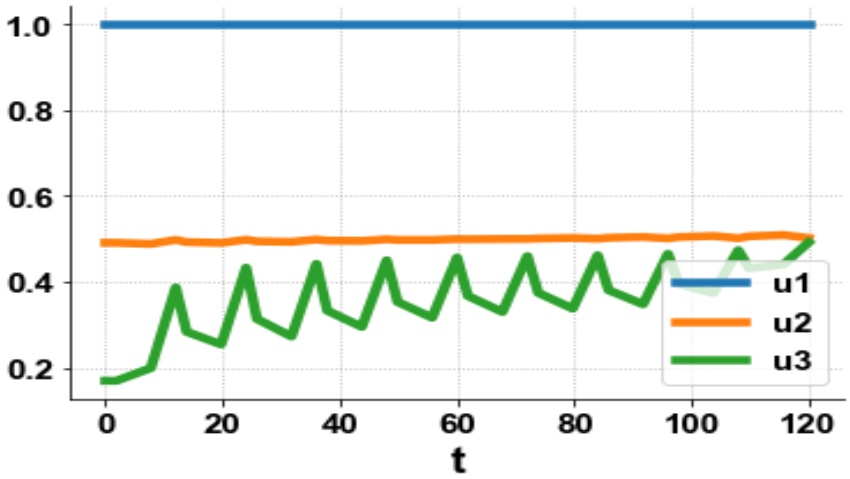

Figure 1h: *MNLMPC Zika Model 1 (u1, u2, u3 vs t)(noise exhibited in control profile)*

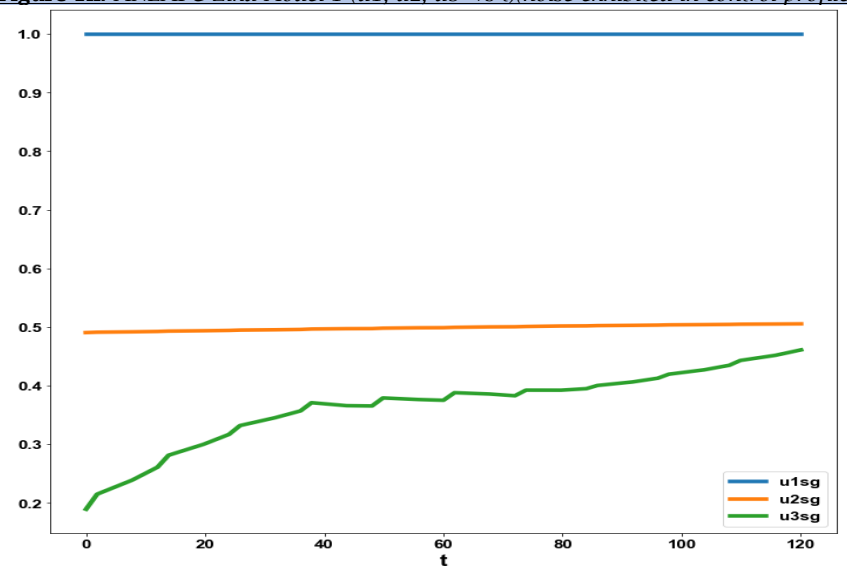

Figure 1i: *MNLMPC Zika Model 1 (u1, u2, u3 vs t)(noise removed in control profile)*

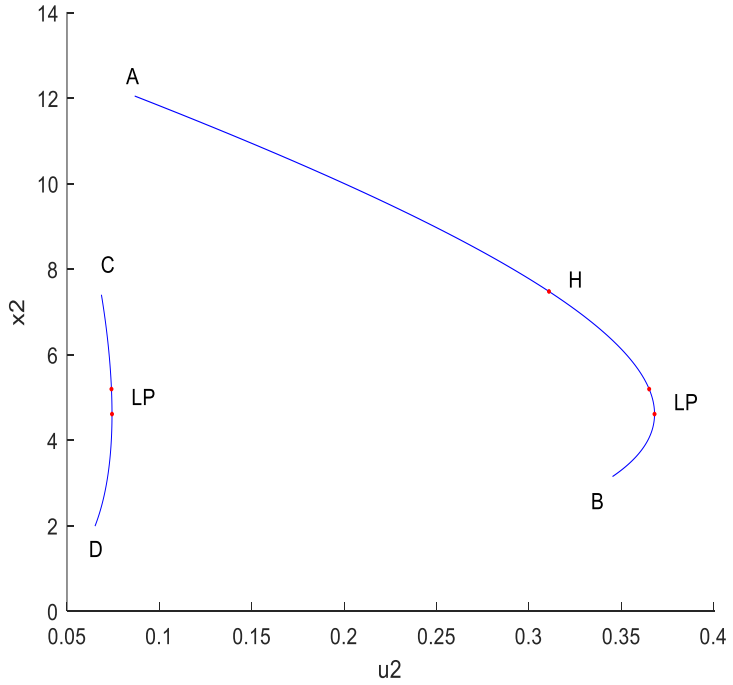

Figure 2a: *Limit point and Hopf bifurcation Point in Zika model 2*

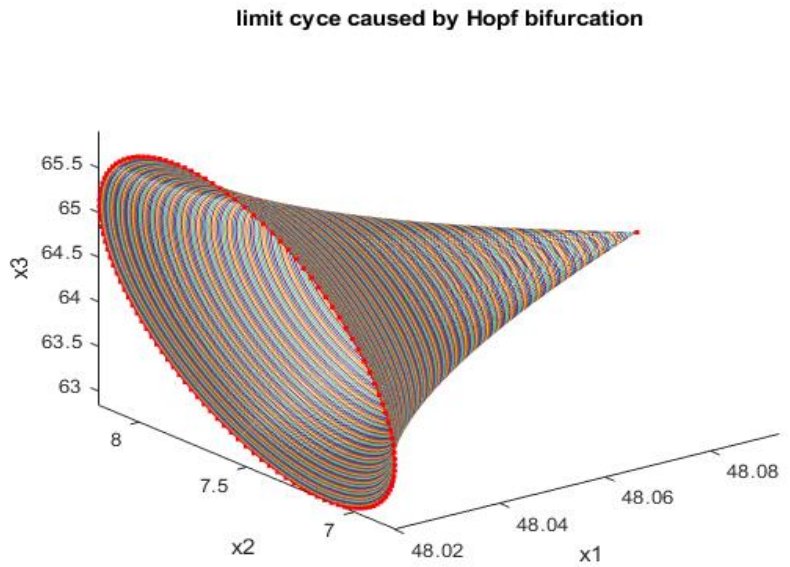

Figure 2b: Limit cycle caused by Hopf bifurcation Point in Zika model 2

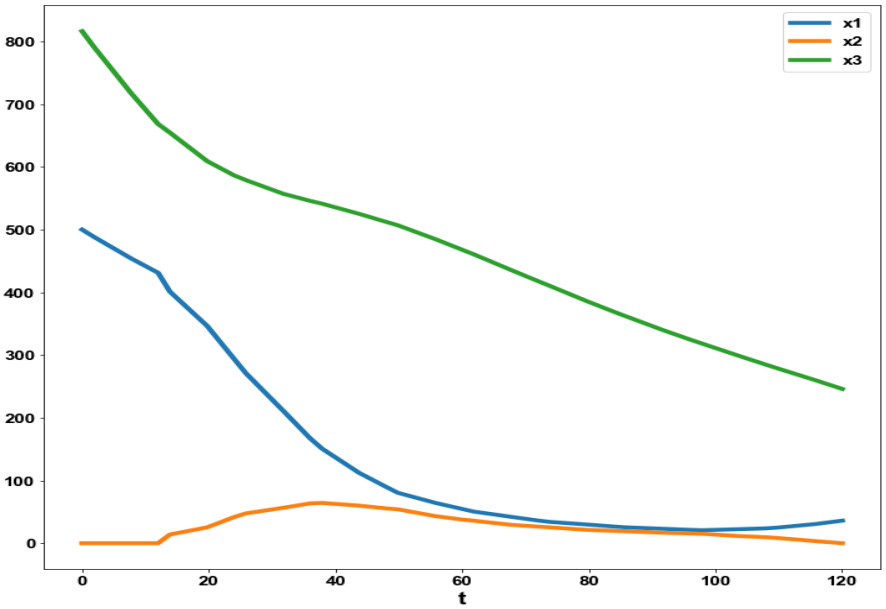

Figure 2c: MNLMC Zika model 2 x1 x2 x3 vs t

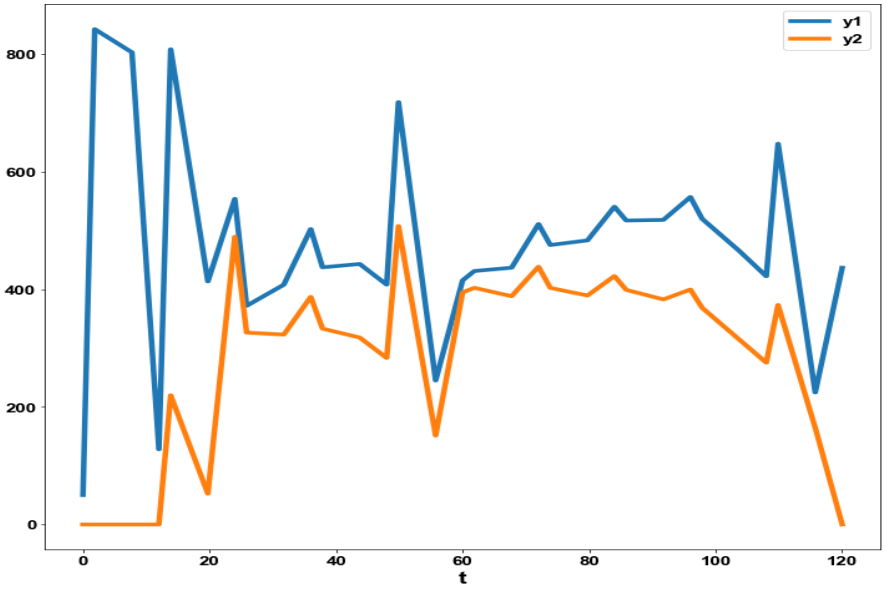

Figure 2d : *MNLMC Zika model 2 y1 y2 vs t*

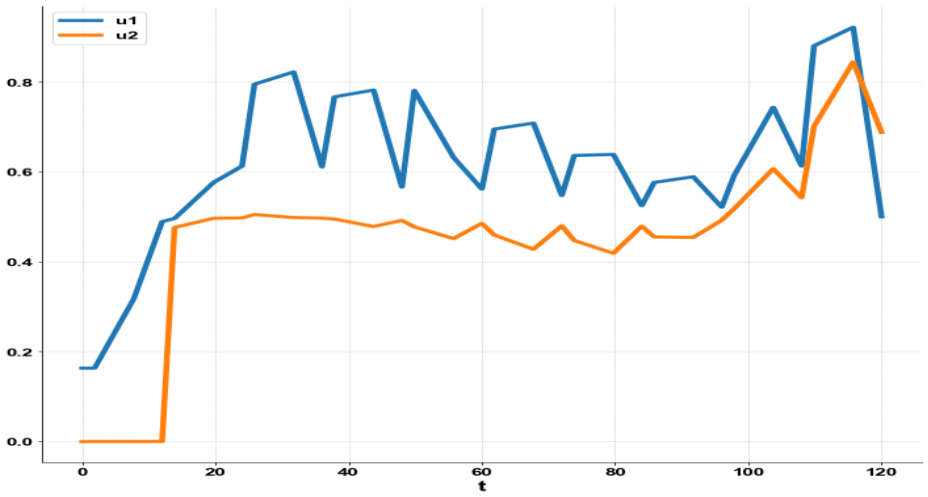

Figure 2e: *MNLMPC Zika Model 2 (u1, u2 vs t)(noise exhibited in control profile)*

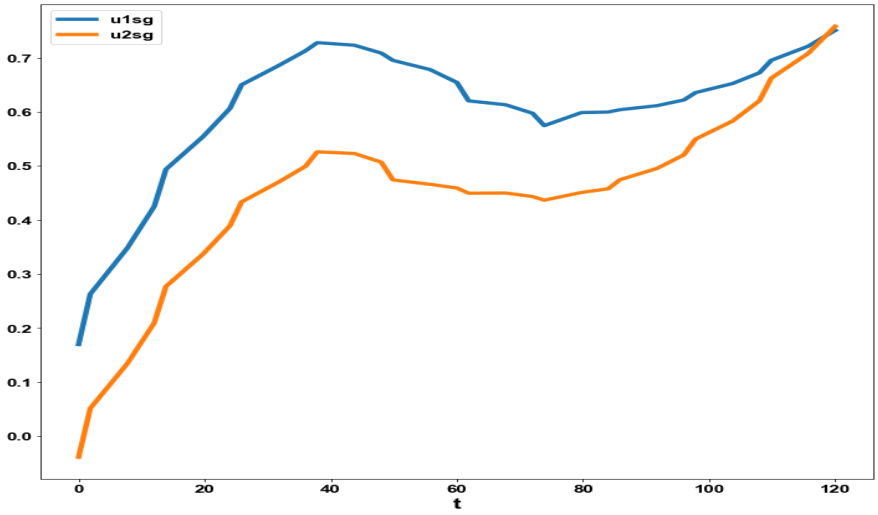

Figure 2f : *MNLMPC Zika Model 1 (u1sg, u2sg)(noise removed in control profile)*

Conclusions

Bifurcation analysis and multiobjective nonlinear control (MNLMPC) studies in two dynamic zika transmission models. The bifurcation analysis revealed the existence of a branch point in the first model and a Hopf bifurcation point and a limit point in the second. The Hopf bifurcation point, which causes an unwanted limit cycle, is eliminated using an activation factor involving the tanh function. The branch and limit points (which cause multiple steady-state solutions from a singular point) are very beneficial because they enable the Multiobjective nonlinear model predictive control calculations to converge to the Utopia point (the best possible solution) in the models. A combination of bifurcation analysis and Multiobjective Nonlinear Model Predictive Control(MNLMPC) for Zika transmission models is the main contribution of this paper.

Data Availability Statement

All data used is presented in the paper

Conflict of interest

The author, Dr. Lakshmi N Sridhar, has no conflict of interest.

Acknowledgement

Dr. Sridhar thanks Dr. Carlos Ramirez and Dr. Suleiman for encouraging him to write single-author papers.

References

1. Duffy, M. R. , T.-H. Chen, W. Thane Hancock, A. M. Powers, J. L. Kool, R. S. Lanciotti, M. Pretrick, M. Marfel, S. Holzbauer, C. Dubray, L. Guillaumot, A. Griggs, M. Bel, A. J. Lambert J. Laven, O. Kosoy, M.S., A. Panella, B. J. Biggerstaff, M. Fischer, E. B. Hayes, Zika virus outbreak on Yap Island, federated states of Micronesia, N. Engl. J. Med., **360** (2009), 2536–2543.

2. Haddow, A. D. A. J. Schuh, C. Y. Yasuda, M. R. Kasper, V. Heang, R. Huy , H. Guzman, R. B. Tesh, S. C. Weaver, Genetic characterization of Zika virus strains: geographic expansion of the Asian lineage, PLOS Negl. Trop. Dis., **6** (2012), 7 pages. 1
3. Oehler, E., L. Watrin, P. Larre, I. Leparc-Goffart, S. Last`ere, F. Valour , L. Baudouin, H. P. Mallet, D. Musso, F. Ghawche, Zika virus infection complicated by Guillain-Barre syndrome–case report, French Polynesia, December 2013, Eurosurveillance, (2014), 3 pages. 1
4. Bewick, S., B., W. F. Fagan, J. Calabrese, F. Agusto, Zika virus: endemic versus epidemic dynamics and implications for disease spread in the Americas, BioRxiv, (2016). 1
5. Perkins, T. A., A. S. Siraj, C. W. Ruktanonchai, M. U. G. Kraemer, A. J. Tatem, Model-based projections of Zika virus infections in childbearing women in the Americas, Nat. Microbiol., **1** (2016), 7 pages 1
6. Bogoch, I. I., O. J. Brady, M. U. G. Kraemer, M. German, M. I. Creatore, M. A. Kulkarni, J. S. Brownstein, S. R. Mekaru, S. I. Hay, E. Groot, A. Watts, K. Khan, Anticipating the international spread of Zika virus from Brazil, The Lancet, **387** (2016), 335–336. 1
7. Bonyah, E., K. O. Okosun, Mathematical modeling of Zika virus, Asian Pac. J. Trop. Dis., **6** (2016), 673–679. 2
8. Brasil, P., J. P. Pereira, Jr., M. E. Moreira, R. M. Ribeiro Nogueira, L. Damasceno, M. Wakimoto, R. S. Rabello, S. G. Valderramos, U.-A. Halai, T. S. Salles, A. A. Zin, D. Horovitz, P. Daltro, M. Boechat, C. Raja Gabaglia, P. Carvalho de Sequeira, J.H. Pilotto, R. Medialdea-Carrera, D. Cotrim da Cunha, L. M. Abreu de Carvalho, M. Pone, A. Machado Siqueira, G.A. Calvet, A.E. Rodrigues Bai˜ao, E.S. Neves, P.R. Nassar de Carvalho, R. H. Hasue, P. B. Marschik, C. Einspieler, C. Janzen, J. D. Cherry, A. M. Bispo de Filippis, K. Nielsen-Saines, Zika virus infection in pregnant women in Rio de Janeiro, N. Engl. J. Med., **375** (2016), 2321–2334.
9. Cao-Lormeau, V.M., . Blake, S. Mons, S. Last`ere, C. Roche, J. Vanhomwegen, T. Dub, Laure Baudouin, A. Teissier, P. Larre, A.-L. Vial, C. Decam, V. Choumet, S. K. Halstead, H. J. Willison, L. Musset, J.-C. Manuguerra, P. Despres, E. Fournier, H.-P. Mallet, D. Musso, A. Fontanet, J. Neil, F. Ghawch´e, Guillain-Barr´e Syndrome outbreak associated with Zika virus infection in French Polynesia: a case-control study, The Lancet, **387** (2016), 1531–1539.
10. Cauchemez, S., M. Besnard, P. Bompard, T. Dub, P. Guillemette-Artur, D. Eyrolle-Guignot, H. Salje, M. D. V. Kerkhove, V. Abadie, C. Garel, A. Fontanet, H.-P. Mallet, Association between Zika virus and microcephaly in French Polynesia, 2013–15: a retrospective study, The Lancet, **387** (2016), 2125–2132.
11. Elsaka, H., E. Ahmed, A fractional order network model for ZIKA, BioRxiv, (2016), 10 pages.
12. Fauci, A. S., D. M. Morens, Zika virus in the Americas—yet another arbovirus threat, N. Engl. J. Med., **374** (2016), 601–604.
13. Gao, D., Y. Lou, D. He, T. C. Porco, Y. Kuang, G. Chowell, S. Ruan, Prevention and control of Zika as a mosquito-borne and sexually transmitted disease: a mathematical modeling analysis, Sci. Rep., **6** (2016), 10 pages.1, 1
14. Heukelbach, J. , C. H. Alencar, A. A. Kelvin, W. K. de Oliveira, L. P. de G´oes Cavalcanti, Zika virus outbreak in Brazil, J. Infect. Dev. Ctries, **10** (2016), 116–120.
15. Kucharski, A. J. , S. Funk, R. M. Eggo, H.-P. Mallet, W. J. Edmunds, E. J. Nilles, Transmission dynamics of Zika virus in island populations: a modelling analysis of the 2013–14 French Polynesia outbreak, PLOS Negl. Trop. Dis., 10 (2016),15 pages. 1
16. Mlakar,J., M. Korva, N. Tul, M. Popovi´c, M. Polj˘sak-Prijatelj, J. Mraz, M. Kolenc, K. Resman Rus, T. Vesnaver Vipotnik, V. Fabjan Vodu˘sek, A. Vizjak, J. Piz˘em, M. Petrovec, T. Avs˘ic˘ Z˘ upanc, Zika virus associated with microcephaly, N. Engl. J. Med., **374** (2016), 951–958.
17. Lee, E. K., Yifan Liu, Ferdinand H. Pietz, A compartmental model for zika virus with dynamic human and vector populations, in: AMIA Annual Symposium Proceedings, Vol. 2016, American Medical Informatics Association, 2016, p. 743.
18. Kibona, I. E. , C.Yang, SIR model of spread of Zika virus infections: ZIKV linked to microcephaly simulations, Health, **9,** (2017), 1190–1210. 2

19. Boret, S. E. B. , R. Escalante, M. Villasana, Mathematical modelling of zika virus in Brazil, arXiv preprint arXiv:1708.01280, (2017), 26 pages. 2
20. Moreno, V. M., B. Espinoza, D. Bichara, S. A. Holechek, C. Castillo-Chavez, Role of short-term dispersal on the dynamics of Zika virus in an extreme idealized environment, Infect. Dis. model., 2 (2017), 21–34. 1
21. Folashade B. Agusto, S. Bewick, W.F. Fagan, Mathematical model of zika virus with vertical transmission, Infec. Dis. Model. 2 (2) (2017) 244–267.
22. Suparit, P., A. Wiratsudakul, C. Modchang, A mathematical model for Zika virus transmission dynamics with a time-dependent mosquito biting rate, Theor. Biol. Med. Model., **15** (2018), 11 pages. 1
23. Wiratsudakul, A., P. Suparit, C. Modchang, Dynamics of Zika virus outbreaks: an overview of mathematical modelling approaches, Peer J, **6** (2018), 30 pages. 1, 2
24. Terefe, Y.A. , H. Gaff, M. Kamga, L. van der Mescht, Mathematics of a model for zika transmission dynamics, Theory Biosci. 137 (2) (2018) 209–218.
25. Blanka Tesla, Leah R. Demakovsky, Erin A. Mordecai, Sadie J. Ryan, Matthew H. Bonds, Calistus N. Ngonghala, Melinda A. Brindley, Courtney C. Murdock, Temperature drives zika virus transmission: evidence from empirical and mathematical models, bioRxiv (2018) 259531.
26. Khan, M. A., Syed Wasim Shah, Saif Ullah, J.F. Gómez-Aguilar,A dynamical model of asymptomatic carrier zika virus with optimal control strategies, Nonlinear Analysis: Real World Applications, Volume 50, 2019, Pages 144-170, ISSN 1468-1218, https://doi.org/10.1016/j.nonrwa.2019.04.006.
27. Denu, D., Son, H.. "Analysis and optimal control of a deterministic Zika virus model." Journal of Nonlinear Sciences and Applications, 15, no. 2 (2022): 88—108
28. Dhooge, A., Govearts, W., and Kuznetsov, A. Y., MATCONT: “A Matlab package for numerical bifurcation analysis of ODEs”, *ACM transactions on Mathematical software* 29(2) pp. 141-164, 2003.
29. Dhooge, A.,W. Govaerts; Y. A. Kuznetsov, W. Mestrom, and A. M. Riet , “CL_MATCONT”; *A continuation toolbox in Matlab,* 2004.
30. Kuznetsov,Y.A. “Elements of applied bifurcation theory” .*Springer,*NY, 1998.
31. Kuznetsov,Y.A.(2009).”Five lectures on numerical bifurcation analysis” ,*Utrecht University,*NL., 2009.
32. Govaerts, w. J. F., “Numerical Methods for Bifurcations of Dynamical Equilibria”, *SIAM*, 2000.
33. Dubey S. R. Singh, S. K. & Chaudhuri B. B. 2022 Activation functions in deep learning: A comprehensive survey and benchmark. *Neurocomputing*, *503*, 92-108. https://doi.org/10.1016/j.neucom.2022.06.111
34. Kamalov A. F. Nazir M. Safaraliev A. K. Cherukuri and R. Zgheib 2021, "Comparative analysis of activation functions in neural networks," *2021 28th IEEE International Conference on Electronics, Circuits, and Systems (ICECS)*, Dubai, United Arab Emirates, , pp. 1-6, doi:10.1109/ICECS53924.2021.9665646.
35. Szandała, T. 2020, Review and Comparison of Commonly Used Activation Functions for Deep Neural Networks. *ArXiv.* https://doi.org/10.1007/978-981-15-5495-7
36. Sridhar. L. N. 2023 Bifurcation Analysis and Optimal Control of the Tumor Macrophage Interactions. *Biomed J Sci & Tech Res* 53(5). BJSTR. MS.ID.008470.**DOI:** 10.26717/BJSTR.2023.53.008470
37. Sridhar LN. Elimination of oscillation causing Hopf bifurcations in engineering problems. Journal of Applied Math. 2024b; 2(4): 1826.
38. Flores-Tlacuahuac, A. Pilar Morales and Martin Riveral Toledo; “Multiobjective Nonlinear model predictive control of a class of chemical reactors” . *I & EC research*; 5891-5899, 2012.
39. Hart, William E., Carl D. Laird, Jean-Paul Watson, David L. Woodruff, Gabriel A. Hackebeil, Bethany L. Nicholson, and John D. Siirola. “Pyomo – Optimization Modeling in Python” Second Edition. Vol. 67.
40. Wächter, A., Biegler, L. “On the implementation of an interior-point filter line-search algorithm for large-scale nonlinear programming”. *Math. Program.* **106**, 25–57 (2006). https://doi.org/10.1007/s10107-004-0559-y
41. Tawarmalani, M. and N. V. Sahinidis, “A polyhedral branch-and-cut approach to global optimization”, *Mathematical Programming*, 103(2), 225-249, 2005

42. Sridhar LN. (2024)Coupling Bifurcation Analysis and Multiobjective Nonlinear Model Predictive Control. Austin Chem Eng. 2024; 10(3): 1107.
43. Upreti, Simant Ranjan(2013); Optimal control for chemical engineers. Taylor and Francis.